Liquid crystal director fluctuations and surface anchoring by molecular simulation

Denis Andrienko,[1] Guido Germano,[1,2] and Michael P. Allen[1]
[1]*H. H. Wills Physics Laboratory, University of Bristol, Royal Fort, Tyndall Avenue, Bristol BS8 1TL, United Kingdom*
[2]*Fakultät für Physik, Universität Bielefeld, 33615 Bielefeld, Germany*
(Received 2 June 2000)

We propose a simple and reliable method to measure the liquid crystal surface anchoring strength by molecular simulation. The method is based on the measurement of the long-range fluctuation modes of the director in confined geometry. As an example, molecular simulations of a liquid crystal in slab geometry between parallel walls with homeotropic anchoring have been carried out using the Monte Carlo technique. By studying different slab thicknesses, we are able to calculate separately the position of the elastic boundary condition and the extrapolation length.

PACS number(s): 61.30.Cz, 61.20.Ja, 07.05.Tp, 68.45.−v

I. INTRODUCTION

Liquid crystal anchoring effects have been intensively studied both experimentally and theoretically during recent decades [1,2]. Such an interest is easily understood since most liquid crystal devices are cells comprising orienting surfaces with a liquid crystal between. Typically, aligning surfaces provide a uniform orientation of the liquid crystal director in the cell interior.

On the phenomenological level, liquid crystal anchoring can be described by two basic parameters: the easy axis direction **e** and the anchoring coefficient W. These two parameters are critical design parameters for every liquid crystal device [3]. A variety of *experimental* methods have been proposed to measure anchoring parameters, in particular the anchoring coefficient W [4,5]. Most of them measure surface director deviations in an external field and involve rather complicated optical setups.

In spite of the practical importance, the mechanism of the director alignment is still not well understood. Experimental techniques always involve optical measurements. They test the entire liquid crystal cell and therefore cannot provide a satisfactory description of the thin interface region. Theoretical investigations of anchoring are also quite controversial. For example, the usual continuous phenomenological theory has divergent surface terms in the elastic free energy expansion [6,7].

One of the approaches for the systematic investigation of anchoring phenomena is computer simulation of liquid crystals in confined geometries. Indeed, computer simulation is a well established method to treat bulk elastic coefficients [8,9], the surface anchoring strength [10], and structures of disclination cores [11,12]. This means that computer simulation allows investigation of details of the liquid crystalline structure that cannot be resolved experimentally.

Several papers have already been published on the search for reasonable surface potentials to use in simulations [13–18]. However, most of them do not characterize aligning surfaces using well established parameters. Questions about the formation of a solid interface layer and values of the easy axis angle and anchoring coefficient are still open. The reason for this is probably a lack of reliable methods to measure these parameters by computer simulation.

In this paper, we propose a technique to measure the surface anchoring strength W by computer simulation. The method itself is based on the study of the *director fluctuations* in the liquid crystal cell. A similar approach has already been used for the *experimental* characterization of the interface [19] and is based on measuring the light scattering caused by the director fluctuations. In computer simulation, the director fluctuations can be studied directly, using ensemble averages of functions of the second-rank order tensor components. A fit to the fluctuation amplitudes with equations predicted by elastic theory then allows determination of the surface anchoring strength.

II. THEORY

Large length- and time-scale fluctuations of the director $\mathbf{n}(\mathbf{r})$ can be described in the continuum model of liquid crystals, based on the phenomenological elastic constants. In this approach, the hydrodynamic equations for the director and the boundary conditions can be obtained by minimization of the cell free energy [20]:

$$F = F_{\mathrm{h}} + F_{\mathrm{b}} + F_{\mathrm{s}}, \tag{1}$$

where $F_{\mathrm{h}} = \frac{1}{2}\gamma(\partial\mathbf{n}/\partial t)^2$ is a hydrodynamic term with an effective viscosity coefficient γ, F_{b} is the Frank elastic free energy, and F_{s} is the surface anchoring energy.

In what follows we use the one-elastic-constant approximation, i.e., $K_{11}=K_{22}=K_{33}=K$. Then the Frank free energy can be brought into the form

$$F_{\mathrm{b}} = \frac{1}{2}K\int_V [(\boldsymbol{\nabla}\cdot\mathbf{n})^2 + (\boldsymbol{\nabla}\times\mathbf{n})^2]d\mathbf{r}.$$

The liquid crystal cell is bounded by surfaces $z=0,L$ which provide some kind of anchoring condition [1]. Below we consider *homeotropic* anchoring, that is, normal to the surface. *Planar* anchoring can be treated in the same way. We assume that the interaction of the director with the cell surfaces has the Rapini-Papoular form [21]

$$F_{\mathrm{s}} = -\frac{1}{2}W\int_{S_0,S_L} (\mathbf{n}\cdot\mathbf{e}_{0,L})^2 d\mathbf{r}_{\perp},$$

where the unit vectors $\mathbf{e}_{0,L}$ define the directions of the easy axes at $z=0,L$: $\mathbf{e}_0=\mathbf{e}_z$, $\mathbf{e}_L=-\mathbf{e}_z$; W is the anchoring energy, and $\mathbf{r}_\perp=(x,y)$.

Equations for the director and boundary conditions can be obtained by minimization of the cell free energy Eq. (1). In the case of homeotropic anchoring on both surfaces the stationary director distribution in the cell is homeotropic, i.e., $\mathbf{n}_0=\mathbf{e}_z$. Therefore, we have to investigate small perturbations of the director around the distribution:

$$\mathbf{n}(\mathbf{r})=\mathbf{n}_0+\delta\mathbf{n}(\mathbf{r}). \tag{2}$$

Minimizing the total free energy (1) and linearizing the equations for the director and boundary conditions with respect to $\delta\mathbf{n}$, we obtain the equations

$$\gamma\frac{\partial}{\partial t}\delta\mathbf{n}=K\nabla^2\delta\mathbf{n} \tag{3}$$

and boundary conditions

$$W\delta\mathbf{n}\pm K\frac{\partial}{\partial z}\delta\mathbf{n}\bigg|_{z=L,0}=\mathbf{0} \tag{4}$$

for the fluctuations. Taking into account Eq. (2), the expression for the free energy fluctuations can be rewritten in the form of the average of the self-conjugate (Hermitian) operator $-\frac{1}{2}K\nabla^2$:

$$\delta F_{\mathrm{b}}=-\frac{1}{2}K\int_V \delta\mathbf{n}(\mathbf{r})\cdot\nabla^2\delta\mathbf{n}(\mathbf{r})d\mathbf{r}. \tag{5}$$

The eigenfunctions of the operator $-\frac{1}{2}K\nabla^2$, which satisfy boundary conditions (4), form a complete set of orthogonal functions characterized by wave vector $\mathbf{q}$. Therefore, $\delta\mathbf{n}(\mathbf{r})$ can be expanded in a series of these orthogonal functions:

$$\delta\mathbf{n}(\mathbf{r})=\frac{1}{V}\sum_{\mathbf{q}_\perp,q_z} e^{i\mathbf{q}_\perp\cdot\mathbf{r}_\perp}[\,\delta\mathbf{n}^{(+)}(\mathbf{q}_\perp,q_z)e^{iq_zr_z} + \delta\mathbf{n}^{(-)}(\mathbf{q}_\perp,q_z)e^{-iq_zr_z}], \tag{6}$$

where $\mathbf{q}_\perp=(q_x,q_y)$ and

$$\delta\mathbf{n}^{(-)}=\frac{i\chi-\xi}{i\chi+\xi}\delta\mathbf{n}^{(+)}. \tag{7}$$

Here we have introduced the dimensionless wave vector $\chi=q_zL$ and anchoring parameter

$$\xi=\frac{WL}{K}=\frac{L}{\lambda}, \tag{8}$$

where λ is the extrapolation length [20]. The wave vectors q_z form a discrete spectrum because of confinement in the z direction which depends on the anchoring energy W (see the Appendix for details). The explicit form of the q_z spectrum is given by the secular equation:

$$(\xi^2-\chi^2)\sin\chi+2\xi\chi\cos\chi=0. \tag{9}$$

Each individual mode can now be seen from Eq. (3) to relax exponentially with a relaxation time given by

$$\tau=\gamma/K(\mathbf{q}_\perp^2+q_z^2). \tag{10}$$

Substituting expansion (6) into the free energy (5) and performing the integration over the cell volume we obtain

$$\delta F_{\mathrm{b}}=\frac{K}{V}\sum_{\mathbf{q}_\perp,q_z}\frac{q^2(2\xi+\chi^2+\xi^2)}{(i\chi+\xi)^2} \times\delta\mathbf{n}^{(+)}(\mathbf{q}_\perp,q_z)\cdot\delta\mathbf{n}^{(+)}(-\mathbf{q}_\perp,q_z).$$

Integrating, we took into account the orthogonality of the eigenfunctions in the expansion (6) with different eigenvectors $\mathbf{q}$, which allowed us to reduce the summations over $\mathbf{q},\mathbf{q}'$ to a single sum over $\mathbf{q}$.

Application of the equipartition theorem of classical statistical mechanics, just as for elastic fluctuations in bulk liquid crystals [22], gives the fluctuation amplitudes

$$\langle\delta\mathbf{n}^{(+)}(\mathbf{q}_\perp,q_z)\cdot\delta\mathbf{n}^{(+)}(-\mathbf{q}_\perp,q_z)\rangle=-\frac{k_{\mathrm{B}}TV(i\chi+\xi)^2}{2Kq^2(2\xi+\chi^2+\xi^2)},$$

where $\langle\cdots\rangle$ denotes an ensemble average.

In molecular simulations, rather than measuring director fluctuations, it is more convenient to measure fluctuations of the second-rank order tensor components (following Forster [22]). We define the real-space order tensor density

$$Q_{\alpha\beta}(\mathbf{r})=\frac{V}{N}\sum_i \delta(\mathbf{r}-\mathbf{r}_i)Q^i_{\alpha\beta},$$

$$Q^i_{\alpha\beta}=\frac{3}{2}\left(u_{i\alpha}u_{i\beta}-\frac{1}{3}\delta_{\alpha\beta}\right),$$

where $\alpha,\beta=x,y,z$, in terms of the orientation vectors $\mathbf{u}_i$ of each molecule i (we consider only uniaxial molecules). If we assume that there is no variation in the *degree* of ordering, we may write

$$Q_{\alpha\beta}(\mathbf{r})=\frac{3}{2}Qn_\alpha(\mathbf{r})n_\beta(\mathbf{r})-\frac{1}{2}Q\delta_{\alpha\beta}$$

where Q is the order parameter, i.e., the largest eigenvalue of $Q_{\alpha\beta}(\mathbf{r})$. If the director $\mathbf{n}_0$ is taken to lie along the z axis throughout the sample, the off-diagonal components $Q_{\alpha z}(\mathbf{r})$, $\alpha=x,y$, are proportional to the fluctuations of the corresponding director components:

$$Q_{\alpha z}(\mathbf{r})=\frac{3}{2}Q\delta n_\alpha(\mathbf{r}).$$

This is the situation for homeotropic anchoring at both surfaces. For planar anchoring, with the director along x and the surface normal along z, the components Q_{xy},Q_{xz} are important (and nonequivalent).

Measurements are performed directly in reciprocal space. The Fourier transform of the real-space order tensor is

$$Q_{\alpha\beta}(\mathbf{k})=\int_V Q_{\alpha\beta}(\mathbf{r})e^{i\mathbf{k}\cdot\mathbf{r}}d\mathbf{r}=\frac{V}{N}\sum_i Q^i_{\alpha\beta}e^{i\mathbf{k}\cdot\mathbf{r}_i}.$$

Then the fluctuations $\langle|Q_{\alpha\beta}(\mathbf{k})|^2\rangle$ can be easily measured from simulations:

$$|Q_{\alpha\beta}(\mathbf{k})|^2=\frac{V^2}{N^2}\left[\left(\sum_i Q^i_{\alpha\beta}\cos(\mathbf{k}\cdot\mathbf{r}_i)\right)^2+\left(\sum_i Q^i_{\alpha\beta}\sin(\mathbf{k}\cdot\mathbf{r}_i)\right)^2\right]. \tag{11}$$

We explicitly relate simulation-measured fluctuation modes with theoretically predicted amplitudes of the director fluctuations for $\mathbf{q}_\perp=\mathbf{0}$,

$$Q_{\alpha z}(k_z)=\frac{3}{2i}Q\sum_{q_z}\delta n^{(+)}_\alpha(\mathbf{0},q_z)\times\left[\frac{e^{i(\kappa+\chi)}-1}{\kappa+\chi}+\left(\frac{i\chi-\xi}{i\chi+\xi}\right)\frac{e^{i(\kappa-\chi)}-1}{\kappa-\chi}\right]$$

where $\kappa=k_zL$. Note that the q_z take discrete (but not equally spaced) values as discussed earlier, while the k_z values are unrestricted.

Since $\delta\mathbf{n}(\mathbf{r})$ is real, using Eq. (6) we have

$$[\,\delta\mathbf{n}^{(+)}(\mathbf{q}_\perp,q_z)]^*=-\frac{\xi^2+\chi^2}{(\xi+i\chi)^2}\delta\mathbf{n}^{(+)}(-\mathbf{q}_\perp,q_z).$$

Taking this equation into account, and the fact that fluctuations with different wave vectors are independent, i.e., $\langle\delta\mathbf{n}^{(+)}(\mathbf{q}_\perp,q_z)\delta\mathbf{n}^{(+)}(-\mathbf{q}_\perp,q_z')\rangle=0$ if $q_z\neq q_z'$, the corresponding ensemble average of the squared order parameter can be rewritten as

$$\langle|Q_{\alpha z}(k_z)|^2\rangle=\frac{9}{8}k_BT\frac{Q^2V}{K}\sum_{q_z}\frac{\chi^2+\xi^2}{q_z^2(2\xi+\chi^2+\xi^2)}\times\left|\frac{e^{i(\kappa+\chi)}-1}{\kappa+\chi}+\left(\frac{i\chi-\xi}{i\chi+\xi}\right)\frac{e^{i(\kappa-\chi)}-1}{\kappa-\chi}\right|^2. \tag{12}$$

We measure Q and $\langle|Q_{\alpha z}(k_z)|^2\rangle$ from simulations, Eq. (11), and then compare with the theoretical prediction Eq. (12), which is parametrized by L, λ, and K. Both the permitted q_z spectrum and the variation of $\langle|Q_{\alpha z}(k_z)|^2\rangle$ with k_z are sensitive to the anchoring strength parameter $\xi=L/\lambda$.

The fluctuation amplitudes given by Eq. (12) have features that simplify the fitting procedure. First, terms with small q_z values dominate because of the q_z^2 in the denominator. Therefore, it is always possible to truncate this sum and use only the first values of the q_z spectrum. Then, for large k_z or for $\kappa\gg\chi$, Eq. (12) can be simplified so that the dependence on k_z is explicit:

$$\langle|Q_{\alpha z}(k_z)|^2\rangle=\frac{9}{2}k_BT\frac{Q^2V}{K}\left[\frac{\sin(\kappa/2)}{\kappa/2}\right]^2\sum_{q_z}\frac{\chi^2}{q_z^2(2\xi+\chi^2+\xi^2)}. \tag{13}$$

Hence, for large k_z, the fluctuation amplitude $\langle|Q_{\alpha z}(k_z)|^2\rangle$ has a characteristic oscillation with the period given by $\kappa=k_zL=2\pi$. This means that we can adjust the cell thickness L independently of parameters λ and K by examining the characteristic wavelength of the fluctuation amplitude $\langle|Q_{\alpha z}(k_z)|^2\rangle$.

III. MOLECULAR MODEL AND SIMULATION METHODS

To test the technique proposed, we simulated a liquid crystal confined between parallel walls (slab geometry), with finite homeotropic anchoring at the walls. The director fluctuations occur around the preferred, *uniform* alignment perpendicular to the walls.

We performed Monte Carlo (MC) simulation of the liquid crystal system. We used a molecular model that has been studied earlier in this geometry [10]. The molecules in this study were modeled as hard ellipsoids of revolution of elongation $e=a/b=15$, where a is the length of the semimajor axis and b the length of the two equal semiminor axes. The phase diagram and properties of this family of models are well studied [23–27]. It is useful to express the density as a fraction of the close-packed density ρ_{cp} of perfectly aligned hard ellipsoids, assuming an affinely transformed face-centered cubic or hexagonal close-packed lattice. In this case, the isotropic-nematic phase transition occurs at quite a low density, $\rho/\rho_{cp}\approx0.2$, and the simulations are performed at a state point corresponding to $\rho/\rho_{cp}\approx0.28$, for which the nematic order parameter is $Q\approx0.85$. For this model, temperature is not a significant thermodynamic quantity, so it is possible to choose $k_BT=1$ throughout.

The slab geometry is defined by two hard parallel confining walls, which cannot be penetrated by the *centers* of the ellipsoidal molecules. Packing considerations generate homeotropic ordering at the surface. Surface anchoring in this system has been studied recently [10] for a system with wall separation $L_z=125b=8.33a$, by applying an orienting perturbation at one of the walls and observing the response at the other. This yielded an estimate of the extrapolation length $\lambda\approx35b\approx2.33a$. In the current work, simulations were carried out for systems of $N=2000$ particles with wall separations $L_z=6.58a,8.22a,9.86a$, which (from the above estimate of λ) would correspond to surface anchoring parameters in the range $2.8\leqslant\xi\leqslant4.2$.

To be sure that we have the same state point for each simulation, we adjusted the density to have the same P_{zz} component of the pressure tensor for all systems. Then a sequence of runs was carried out using the constant-NVT ensemble, allowing typically 10^5 MC sweeps for equilibration and 10^7 sweeps for accumulation of averages (one sweep is one attempted move per particle).

IV. SIMULATION RESULTS AND DISCUSSION

The simulation results were analyzed to give a density profile and an order tensor profile which are shown in Figs. 1 and 2. From these profiles we can see that the walls are sufficiently well separated, and the variation of the order parameter across the slab is small, even in spite of the large change in local density near the walls.

The order tensor fluctuations in reciprocal space were calculated using expression (11). To fit the simulation results with the elastic theory we have to remember that the size of the simulation box L_z is not necessarily equal to the liquid

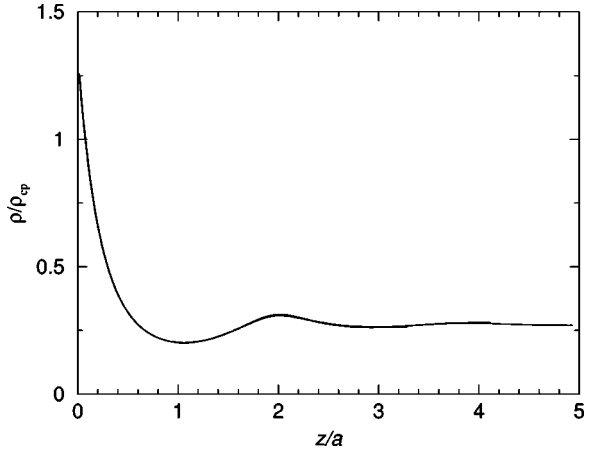

FIG. 1. Density profiles as functions of z-coordinate. Distances are normalized by the molecular semiaxis length a and the density is expressed relative to the closed-packed density ρ_{cp} for perfectly aligned ellipsoids. The profiles are symmetrical; only one side of the slab is shown. The results for different wall separations are almost indistinguishable on this scale.

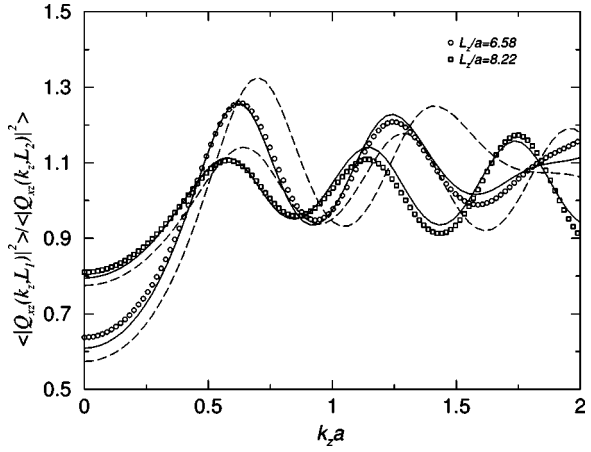

FIG. 3. Ratio of the director fluctuations as function of wave vector (normalized by the molecular semiaxis length a) for different wall separations. Symbols: Monte Carlo results; solid lines: elastic theory dashed lines: elastic theory without correction for the difference between the elastic-theory cell thickness L and the simulation box size L_z.

crystal cell thickness L appearing in the elastic theory. The former is a physical quantity, which, in statistical mechanics, is determined by the positions at which the liquid number density becomes identically zero. The latter appears in the elastic theory: it is determined by the positions at which the orientational elastic boundary conditions are applied. Physically, the difference may be ascribed to partial penetration of the walls by the liquid crystal molecules, formation of an ordered (or solid) layer near the walls, or other molecular-scale features. We assume that we may write $L=L_z+2L_{\mathrm{w}}$, where the value L_{w} (which may be positive or negative) is characteristic of the wall, independent of L_z, and may be determined in our fitting process.

The best estimate of the wall-induced separation distance L_{w} was obtained by examining the ratios $\langle|Q_{\alpha z}(k_z,L_1)|^2\rangle/\langle|Q_{\alpha z}(k_z,L_2)|^2\rangle$ for different $L_{1,2}$ since they reveal more structure for large k_z. Plotting the results in this way removes the overall scaling of the amplitudes of fluctuations, which are sensitive to changes in λ, while the shapes of the curves, and the characteristic oscillation wavelengths, are sensitive to the choice of L_{w}. These ratios with $L_1=6.58a, 8.22a$, $L_2=9.86a$, and corresponding fitting curves are plotted in Fig. 3. The best fits were obtained with $L_{\mathrm{w}}/a=0.59$. In this figure we also plot theoretical curves with $L_{\mathrm{w}}=0$: the clear discrepancy with the simulation results indicates that the simulation box size L_z is indeed significantly different from the actual cell thickness.

Following the determination of L_{w}, we adjusted the extrapolation length λ to obtain the best fit to the fluctuation data: the fluctuation amplitudes with small k_z are most sensitive to this quantity. Together with the corresponding fitting curves for the different slab thicknesses, our results are plotted in Fig. 4. The best fits were obtained with a bulk

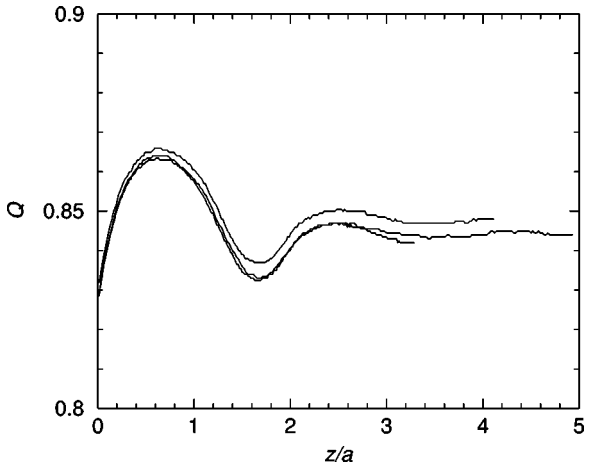

FIG. 2. Profiles of nematic order parameter Q for different wall separations. Distances are normalized by the molecular semiaxis length a. The profiles are symmetrical; only one side of the slab is shown. Note the highly expanded vertical scale.

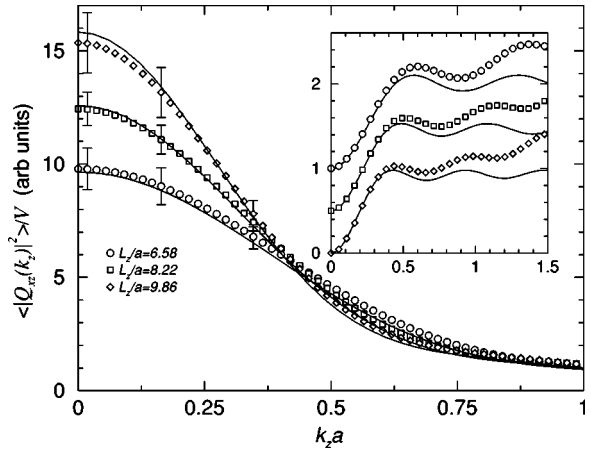

FIG. 4. Director fluctuations (arbitrary units) as function of wave vector (normalized by the molecular semi axis length a) for different wall separations. Symbols: Monte Carlo results. Error estimates are indicated at some representative points; at higher wave vectors the errors are smaller than the plotting symbols. Solid lines: elastic theory, fitted to parameters discussed in the text. Inset: fluctuations multiplied by $(k_za)^2$ to emphasize structure at higher wave numbers. Successive curves are offset by 0.5 for clarity.

elastic constant $Ka/k_BT \approx 66$ and an extrapolation length $\lambda/a \approx 2.3$. The theoretical fitting curves agree well with the simulation results, for small values of k_z, as one would expect for a theory valid for long-wavelength fluctuations. At higher k_z, the structure (emphasized in the inset of Fig. 4 by a multiplying factor k_z^2) is not perfectly reproduced, but the agreement is satisfactory. This is not surprising, since we expect the elastic theory to become less accurate at higher k_z. Finally, we note that the extrapolation distance relative to the simulation wall position is $L_w + \lambda \approx 2.89a$, which compares moderately well with the value $\lambda \approx 2.33a$ obtained in the previous study of this system [28]. It should be noted that the director configuration of that work does not allow one to determine, separately, L_w and λ, so the quoted value of λ really represents $\lambda + L_w$.

We have to point out some possible limitations of the method. The first one is computational time. The effect of the surfaces is to dampen the amplitude of long-wavelength modes; these have the longest relaxation times, according to Eq. (10), and so it is essential to carry out very long runs to adequately sample them. We have paid some attention to estimating the error bars on the measured values of $|Q_{\alpha z}(k_z)|^2$, as indicated in Fig 4: the larger values at low k_z follow directly from this effect. We shall return to examine the time dependence of fluctuations in a future publication. The second limitation is the actual sensitivity of the measured averages to the variation in the anchoring strength and cell thickness. One might expect that in practice it is not possible to measure large values of the anchoring parameter $\xi = L_z/\lambda$, so we need reasonably thin cells. As the cell thickness L_z becomes large, the fluctuation spectrum becomes insensitive to L_w. However, it is important that the walls do not become too close: the *bulk* region should be sufficiently large compared to the *interfacial* region. Only in this case can we assume that the scalar order parameter Q in the liquid crystal bulk is constant for large scale fluctuation modes.

To summarize, analysis of the director fluctuations in nematic liquid crystal slabs allowed us to measure the surface anchoring strength parameter. The method has been tested for a system of hard ellipsoids of revolution of elongation $e = 15$ confined between hard walls with homeotropic anchoring. Careful analysis of fluctuations in slabs of different thickness has allowed us to resolve the position of the elastic boundary condition relative to the simulation wall, as well as to measure the extrapolation length. The elastic theory gives a good description at low wave numbers, but is less accurate at higher wave numbers.

ACKNOWLEDGMENTS

This research was supported by EPSRC. D.A. acknowledges support through an Overseas Research Grant; G.G. acknowledges the support of a British Council Grant; M.P.A. is grateful to the Alexander von Humboldt Foundation. Some of this work was carried out while visiting the Max Planck Institute for Polymer Research, Mainz, and the Institute of Physics, University of Mainz; the authors are grateful to Kurt Kremer and Kurt Binder for their hospitality, and conversations with F. Schmid and H. Lange are gratefully acknowledged.

APPENDIX: FLUCTUATION SPECTRUM

To obtain the spectrum of the q_z modes of the fluctuations we need to select from the eigenfunctions of the operator $-\frac{1}{2}K\nabla^2$ those that satisfy the boundary conditions (4). Substituting Eq. (6) into the boundary conditions (4), we obtain a set of linear equations

$$(\xi + i\chi)e^{i\chi}\delta\mathbf{n}^{(+)} + (\xi - i\chi)e^{-i\chi}\delta\mathbf{n}^{(-)} = \mathbf{0},$$

$$(\xi - i\chi)\,\delta\mathbf{n}^{(+)} + (\xi + i\chi)\,\delta\mathbf{n}^{(-)} = \mathbf{0}.$$

This set of linear homogeneous equations for $\delta\mathbf{n}^{(\pm)}$ has a nontrivial solution if its determinant equals zero. This condition leads to the secular equation for the q_z vector (9) and relation (7).

In the case of strong anchoring, $\xi \to \infty$, the q_z spectrum is equidistant: $q_z L = \pi n$, where n is a positive integer. For finite anchoring coefficient ξ, we have a shift in this spectrum. The magnitude of the shift depends on the anchoring parameter ξ. Indeed, for sufficiently strong anchoring parameters, $\xi \gg 1$, asymptotically

$$q_z L = \pi n - \frac{2\pi n}{\xi}, \quad n = 1,2,\ldots, \quad n/\xi \ll 1,$$

which is equivalent to replacing L by $(L + 2\lambda)$, λ being the extrapolation length.

For weak anchoring, $\xi \ll 1$,

$$q_z L = \pi n + \frac{2\xi}{\pi n}, \quad n = 1,2,\ldots,$$

$$q_z L = \xi^{1/2}, \quad n = 0.$$

The spectrum of the q_x, q_y wave vectors depends on the system geometry. Again, if we have periodic boundary conditions in the x and y directions, q_x and q_y have a discrete spectrum on a fine grid $q_\alpha L_\alpha = 2\pi n_\alpha$ ($n_\alpha = 0,1,2,\ldots,$), otherwise $\mathbf{q}_\perp = (q_x, q_y)$ is unrestricted.

It is also easy to show that the eigenfunctions that correspond to different eigenvalues q_z and q_z' are orthogonal. Indeed, using Eq. (7) we can rewrite

$$\Phi(\mathbf{q}_\perp, q_z) = \delta\mathbf{n}^{(+)}(\mathbf{q}_\perp, q_z)e^{iq_z r_z} + \delta\mathbf{n}^{(-)}(\mathbf{q}_\perp, q_z)e^{-iq_z r_z}$$
$$= \frac{2i}{i\chi + \xi}[\chi\cos(q_z z) + \xi\sin(q_z z)]\,\delta\mathbf{n}^{(+)}(\mathbf{q}_\perp, q_z).$$

It is easy to check using the secular equation (9) that functions $\phi(q_z) = \chi\cos(q_z z) + \xi\sin(q_z z)$ are orthogonal, i.e.,

$$\int_0^L \phi(q_z)\,\phi(q_z')\,dz = \frac{1}{2}L(2\xi + \chi^2 + \xi^2)\,\delta_{q_z, q_z'}, \quad \text{(A1)}$$

where $\delta_{q_z, q_z'}$ is the Kronecker delta. Therefore, the eigenfunctions $\Phi(\mathbf{q}_\perp, q_z)$ are orthogonal and can be normalized using Eq. (A1).

[1] B. Jérôme, Rep. Prog. Phys. **54**, 391 (1991).
[2] A. Poniewierski and A. Samborski, Phys. Rev. E **53**, 2436 (1996).
[3] D. Andrienko *et al.*, Liq. Cryst. **27**, 365 (2000).
[4] D.-F. Gu, S. Uran, and C. Rosenblatt, Liq. Cryst. **19**, 427 (1995).
[5] D. Andrienko *et al.*, Mol. Cryst. Liq. Cryst. Sci. Technol., Sect. A **321**, 271 (1998).
[6] V. M. Pergamenshchik, Phys. Rev. E **48**, 1254 (1993).
[7] V. M. Pergamenshchik and S. Zumer, Phys. Rev. E **59**, R2531 (1999).
[8] M. P. Allen and D. Frenkel, Phys. Rev. A **37**, 1813 (1988).
[9] M. P. Allen and D. Frenkel, Phys. Rev. A **42**, 3641(E) (1990).
[10] M. P. Allen, Mol. Phys. **96**, 1391 (1999).
[11] S. D. Hudson and R. G. Larson, Phys. Rev. Lett. **70**, 2916 (1993).
[12] D. Andrienko and M. P. Allen, Phys. Rev. E **61**, 504 (2000).
[13] Z. Zhang, A. Chakrabarti, O. G. Mouritsen, and M. J. Zuckermann, Phys. Rev. E **53**, 2461 (1996).
[14] J. Stelzer, P. Galatola, G. Barbero, and L. Longa, Phys. Rev. E **55**, 477 (1997).
[15] J. Stelzer, L. Longa, and H.-R. Trebin, Phys. Rev. E **55**, 7085 (1997).
[16] T. Gruhn and M. Schoen, Phys. Rev. E **55**, 2861 (1997).
[17] T. Gruhn and M. Schoen, J. Chem. Phys. **108**, 9124 (1998).
[18] G. D. Wall and D. J. Cleaver, Phys. Rev. E **56**, 4306 (1997).
[19] T. Y. Marusii *et al.*, Zh. Éksp. Teor. Fiz. [Sov. Phys. JETP **91**, 851 (1986)].
[20] P. G. de Gennes and J. Prost, *The Physics of Liquid Crystals*, 2nd, paperback ed. (Clarendon Press, Oxford, 1995).
[21] A. Rapini and M. Papoular, J. Phys. Colloq. **30 (C4)**, 54 (1969).
[22] D. Forster, *Hydrodynamic Fluctuations, Broken Symmetry and Correlation Functions*, Vol. 47 of *Frontiers in Physics* (Benjamin, Reading, MA, 1975).
[23] D. Frenkel, B. M. Mulder, and J. P. McTague, Phys. Rev. Lett. **52**, 287 (1984).
[24] D. Frenkel and B. M. Mulder, Mol. Phys. **55**, 1171 (1985).
[25] B. Tjipto-Margo, G. T. Evans, M. P. Allen, and D. Frenkel, J. Phys. Chem. **96**, 3942 (1992).
[26] M. P. Allen, in *Understanding Self-Assembly and Organization in Liquid Crystals*, theme issue of Philos. Trans. R. Soc. London, Ser. A **344**, 323 (1993).
[27] M. P. Allen, G. T. Evans, D. Frenkel, and B. Mulder, Adv. Chem. Phys. **86**, 1 (1993).
[28] M. P. Allen, J. Chem. Phys. **112**, 5447 (2000).